# Synergistic antiviral effect of hydroxychloroquine and azithromycin in combination against SARS-CoV-2: What molecular dynamics studies of virus-host interactions reveal

Jacques Fantini, Coralie Di Scala, Henri Chahinian, Nouara Yahi

# Structural and molecular modeling studies reveal a new mechanism of action of chloroquine and hydroxychloroquine against SARS-CoV-2 infection

Jacques Fantini[1], Coralie Di Scala[2], Henri Chahinian[1] and Nouara Yahi[1]

[1]INSERM UMR_S 1072, 13015 Marseille, France; Aix-Marseille Université, 13015 Marseille, France.

[2]INMED, INSERM U1249, Parc Scientifique de Luminy, 163 Avenue de Luminy, BP13 13273 Marseille Cedex 09, France.

**Int J Antimicrob Agents 2020 May;55(5):105960.**

**doi: 10.1016/j.ijantimicag.2020.105960. Epub 2020 Apr 3.**

**Abstract**

The recent emergence of the novel pathogenic SARS-coronavirus 2 (SARS-CoV-2) is responsible for a global pandemic. In face of the health emergency, drug repositioning is the most reliable option to design an efficient therapy for infected patients without delay. The first step of the viral replication cycle, i.e. the attachment to the surface of respiratory cells mediated by the spike (S) viral protein, offers several potential therapeutic targets. The S protein uses the ACE-2 receptor for entry, but also sialic acids linked to host cell surface gangliosides. Using a combination of structural and molecular modeling approaches, we showed that chloroquine (CLQ), one of the drugs currently under investigation for SARS-CoV-2 treatment, binds sialic acids and gangliosides with high affinity. We identified a new type of ganglioside-binding domain at the tip of the N-terminal domain of the SARS-CoV-2 spike (S) protein. This domain (aa 111-158), which is fully conserved among clinical isolates worldwide, may improve the attachment of the virus to lipid rafts and facilitate the contact with the ACE-2 receptor. We showed that in presence of CLQ (or of the more active derivative hydroxychloroquine, CLQ-OH), the viral spike is no longer able to bind gangliosides. The identification of this new mechanism of action of CLQ and CLQ-OH supports the use of these repositioned drugs to cure SARS-CoV-2 infected patients and stop the pandemic. Our in silico approaches might also be used to assess the efficiency of a broad range of repositioned and/or innovative drug candidates before their clinical evaluation.

**Keywords:** coronavirus, pandemic, SARS-CoV-2, ganglioside, spike, chloroquine

**Abbreviations:** ACE-2, angiotensin converting enzyme-2; CLQ, chloroquine; CLQ-OH, hydroxychloroquine; COVID-19, coronavirus disease 19; GBD, ganglioside binding domain; NTD, N-terminal domain; RBD, receptor binding domain; SARS-CoV, severe acute respiratory syndrome coronavirus; SARS-CoV-2, SARS-coronavirus-2

**Funding:** This research did not receive any specific grant from funding agencies in the public, commercial, or not-for-profit sectors.

## 1. Introduction

In face of the COVID-19 pandemic due to the emergence of the new SARS-CoV-2 [1], it is urgent to identify active antiviral compounds that can block the infection at the individual stage and stop its spread over the world. Due to the health emergency, repositioning of approved therapeutic drugs [2] has been suggested to be the most efficient way to find a cure for this virus [3]. Several drugs have already been tested, among which chloroquine (CLQ), a well-known anti-malarial drug, is one of the most promising as it has shown apparent efficacy in treatment of COVID-19 associated pneumonia in recent clinical studies [4]. However, the mechanism of action of CLQ against SARS-CoV-2 is unclear as the drug seems to exert a broad range of potential antiviral effects [5]. Therefore, although CLQ is classically considered as an inhibitor of endocytic pathways through an elevation of endosomal pH [6], its detailed molecular mechanisms of action as an antiviral compound is still an open issue [3, 5]. Interestingly, the drug was also shown to interfere with the terminal glycosylation of angiotensin converting enzyme-2 (ACE-2) [7], which acts a plasma membrane receptor for both SARS-CoV SARS-Cov-2 [8] and SARS-CoV-2 [9]. The authors of this study concluded that CLQ could act at several steps of the coronavirus replication cycle [7]. In any case, these data suggest the interesting and mostly unexplored possibility that CLQ could prevent virus attachment through a direct effect on host cell surface molecules.

One important characteristics of human coronaviruses is that besides their protein membrane receptor, they are also depend upon sialic acid-containing glycoproteins and gangliosides that act as primary attachment factors along the respiratory tract [10]. In this report, we used a combination of structural and molecular modeling approaches [11] to investigate the potential interaction between CLQ and sialic acids. Moreover, we identified a ganglioside-binding site in the N-terminal domain (NTD) of the S glycoprotein of SARS-CoV-2 and we demonstrated that CLQ is a potential blocker of the spike-ganglioside interaction which occurs at the very

first step of the viral infection cycle. Finally, we compared the antiviral potential of CLQ and its derivative hydroxychloroquine (CLQ-OH) against SARS-CoV-2. Overall, these data confirm that CLQ and CLQ-OH might be used to fight pathogenic human coronaviruses [3-6], especially SARS-CoV-2 [12].

## 2. Materials and Methods

In silico analyses were performed using Hyperchem and Molegro Molecular viewer as described [11,13,14]. The initial coordinates of GM1 were obtained from CHARMM-GUI Glycolipid Modeler (http://www.charmmgui.org/?doc=input/glycolipid; [15])
which uses the internal coordinate information of common glycosidic torsion angle values, orients the ganglioside perpendicular to the membrane, and performs Langevin dynamics with a cylindrical restraint potential to keep the whole GM1 molecule cylindrical, especially the membrane-embedded ceramide part. In the next step, we included the ganglioside in a periodic box solvated with 1128 water molecules. The system was energy-minimized 6 times switching alternatively between runs using steepest descent gradients or Polak–Ribière conjugate gradients until convergence to machine precision. The ganglioside was then merged with the NTD domain of SARS-CoV-2 S protein as obtained from pdb file # 6VSB [16]. Initial conditions corresponded to minimized structures obtained with the Polak–Ribière algorithm. Docked complexes were subsequently submitted to iterative cycles of molecular dynamics using the CHARMM36 force field optimized for carbohydrates [17]. Interaction energies were calculated from stable complexes using the Ligand Energy Inspector function of Molegro [13].

N-Acetylneuraminic acid (Neu5Ac) was generated with the Hyperchem database. 9-O-acetyl-N-acetylneuraminic acid (9-O-SIA), was retrieved from pdb file 6Q06 [18]. Chloroquine

(CLQ) is N-(7-chloroquinolin-4-yl)-N,N-diéthyl-pentane-1,4-diamine. Its 3D structure was retrieved from pdb file # 4V2O [19]. Hydroxychloroquine (CLQ-OH) is (RS)-2-[{4-[(7-chloroquinolin-4-yl)amino]pentyl}(ethyl)amino]ethanol. CLQ-OH was generated by hydroxylation of CLQ with Hyperchem. Both CLQ and CLQ-OH were energy minimized and merged with water molecules as described in the Results section.

## 3. Results

### 3.1. Structural and conformational analysis of CLQ and CLQ-OH in water

The chemical structures of CLQ and CLQ-OH are shown in Figure 1a and 1b, respectively. The only difference between both molecules is the presence of a terminal hydroxyl group in CLQ-OH. This OH group has a marked influence on the conformation and the water solubilization properties of the drug. CLQ-OH may adopt a wide range of conformations, the most stable being the extended one shown in Figure 1c. When immersed in a periodic box of 31.5 $Å^2$ with 1042 water molecules, the system reached, at the equilibrium, an energy of interaction estimated to -92 $kJ.mol^{-1}$, accounting for 56 water molecules solvating CLQ-OH (Figure 1d). In contrast, due to and intramolecular hydrophobic effect, CLQ appeared more condensed than CLQ-OH (Figure 1e). At equilibrium, CLQ was surrounded by 58 water molecules with an energy of interaction of -79 $kJ.mol^{-1}$ (Figure 1f).

We used these water compatible conformations of CLQ and CLD-OH as initial conditions for studying the interaction of these drugs with sialic acids and gangliosides.

### 3.2. Sialic acids as molecular targets of CLQ and CLQ-OH

N-Acetylneuraminic acid (Neu5Ac) is the predominant sialic acid found in human glycoproteins and gangliosides. When CLQ was merged with Neu5Ac, a quasi-instantaneous

fit occurred between both molecules whose global shapes in water are complementary geometrically (Figure 2a). This is particularly obvious in the views of the CLQ-Neu5Ac complex in mixed surface/balls & sticks rendition (Figure 2a and 2b). The interaction was driven by the positioning of the negative charge of the carboxylate group of Neu5Ac and one of the two cationic charges of CLQ (pKa 10.2) (Figure 2c). The energy of interaction of this complex was estimated to -47 kJ.mol$^{-1}$. Since coronavirus preferentially interact with 9-O-acetyl-N-acetylneuraminic acid (9-O-SIA) [10], we used a similar molecular modeling approach to assess whether CLQ could also interact with this specific sialic acid. A good fit between CLQ and 9-O-SIA could be obtained (Figure 2d-f), with an energy of interaction of -45 kJ.mol$^{-1}$. In this case, the carboxylate group of the sialic acid interacted with the cationic group of the nitrogen-containing ring of CLQ (pKa 8.1) (Figure 2d). The complex was further stabilized by OH-π and van der Waals interactions.

Then we tested CLQ-OH to assess whether it could, as CLQ, bind to 9-O-SIA (Figure 3). The complex obtained with CLQ-OH was very similar to the one obtained with CLQ (e.g. compare Figure 3a-b with 2e-f), although several conformational adjustments occurred during the simulations. Interestingly, the OH group of CLQ-OH reinforced the binding of CLQ to the sialic acid through the establishment of a hydrogen bond (Figure 3c and 3d). Overall, this hydrogen bond compensated the slight loss of energy consecutive the conformational rearrangement and the energy of interaction of the complex was estimated to -46 kJ.mol$^{-1}$, which is very close to the value obtained for CLQ (-45 kJ.mol$^{-1}$).

### 3.3. Molecular recognition of gangliosides by CLQ and CLQ-OH

In the respiratory tract, sialic acids are usually part of glycoproteins and gangliosides. In order to assess whether CLQ and CLQ-OH can recognize sialic acid units in their natural molecular environment. In these simulations, ganglioside GM1 was chosen as a representative example

of human plasma membrane gangliosides. A first series of simulations was performed with CLQ. When merged with the ganglioside, CLQ could find two distinct binding sites, both located in the polar saccharide part of GM1. The first site was located at the tip of the saccharide moiety of the ganglioside (Figure 4a and 4b). The energy of interaction was estimated to -47 kJ.mol$^{-1}$. CLQ retained the typical L-shape structure of the water-soluble conformer bound to isolated sialic acids (compare Figures 2c and 4a). From a mechanistic point of view, the carboxylate group of the sialic acid of GM1 was oriented towards the cationic groups of CLQ. The rings of CLQ faced the N-acetylgalactosamine (GalNAc) residue of GM1, establishing both OH-Pi interaction and hydrogen bonding (Figure 4b). The second site was in a large area including both the ceramide-sugar junction and the saccharide moiety (Figure 4c). The chlorine atom of CLQ was oriented towards the ceramide axis, allowing the nitrogen-containing ring of CLQ to stack onto the pyrane ring of the first sugar residue, i.e. glucose (Glc). The quite perfect geometric complementarity of both partners (Figure 4c and 4d) accounted for a particularly high energy of interaction in this case, i.e. -61 kJ.mol$^{-1}$. Interestingly, there was no overlapping between both CLQ binding sites on GM1, so that the ganglioside could accommodate two CLQ molecules (Figure 4e), reaching a global energy of interaction of -108 kJ.mol$^{-1}$. A similar situation was observed with CLQ-OH, which occupies the same binding site as CLQ (Figure 4f). In this case, the energy of interaction was further increased by stabilizing contacts established between both CLQ-OH molecules, reaching -120 kJ.mol$^{-1}$. Overall, these data showed that CLQ and CLQ-OH have a good fit for sialic acids, either isolated or bound to gangliosides.

### 3.4. Structural analysis of the NTD of SARS-CoV-2 S protein

The next step of our study was to determine how SARS-CoV-2 could interact with plasma membrane ganglioside and whether such interaction could be affected by CLQ and CLQ-OH.

The global structure of the SARS-CoV-2 spike [16] is shown in Figure 5a-d. It consists in a trimer of S protein, each harboring two distinct domains distant from the viral envelope, i.e. the receptor binding region (RBD) and the N-terminal domain (NTD).

We reasoned that if the RBD is engaged into functional interactions with the ACE-2 receptor, it would be interesting to search for potential ganglioside binding sites on the other cell-accessible domain of the S glycoprotein, i.e. the NTD. The NTD contains ca. 290 amino acid residues. The tip of the NTD particularly retained our attention since it displays a flat interface (Figure 5f) ideally positioned for targeting a ganglioside-rich plasma membrane microdomain, such as a lipid raft.

The amino acid sequence of the planar interfacial surface located at the tip of the NTD was analyzed for the presence of a consensus ganglioside binding domains [20]. These motifs are constituted by a triad of mandatory amino acid residues such as (K,R)-$X_n$-(F,YW)-$X_n$-(K,R). The $X_n$ intercalating segments, usually 4-5 residues, may contain any amino acid but often Gly, Pro and/or Ser residues. The strict application of this algorithm did allow to detect any potential ganglioside binding domain in this region of the NTD. However, there is an intriguing overrepresentation of aromatic and basic residues in the 129-158 segment:

**129-<u>K</u>**VCE**<u>F</u>**Q**<u>F</u>**CNDP**<u>F</u>**LGV**<u>YY</u>**H**<u>K</u>**NN**<u>K</u>**S**<u>W</u>**MESE**<u>FR</u>**-158**

This 30-amino acid stretch also contains Gly, Pro and/or Ser residues that are often found in ganglioside binding motifs. These observations supported the notion that the tip of the NTD could display a large ganglioside attachment interface.

### 3.5. Molecular interactions between ganglioside and the NTD of SARS-CoV-2 S protein

Molecular dynamics simulations of a structural motif encompassing amino acid residues 100 to 175 of the NTD (Figure 5f-h) merged with ganglioside GM1 further supported the concept. As shown in Figure 6, the large flat area of this structural domain fitted very well with the

protruding oligosaccharide part of the ganglioside. Several amino acid residues appeared critical for this interaction, especially Phe-135, Asn-137, and Arg-158 (Table 1). Overall, the complex involved 10 amino acid residues, for a total energy of interaction of -100 $kJ.mol^{-1}$. At this stage, we observed that about 50% of the interface was involved in the complex, leaving the remaining 50% available for an interaction with a second GM1 molecule. As expected, merging a second GM1 molecule with the preformed GM1-NTD complex led to a trimolecular complex consisting of two gangliosides in a typical symmetric chalice-like structure into which the NTD could insert its interfacial ganglioside binding domain (Figure 7). The formation of this trimolecular complex was progressive, starting with a conformational rearrangement of the first ganglioside-NTD complex triggered by the coming of the second GM1 molecule. The energy of interaction of the new complex was consistently increased by 37%, reaching the estimated value of -137 $kJ.mol^{-1}$. At this stage, the attachment of the NTD to the ganglioside-rich microdomain involved the whole interface, i.e. 15 surface-accessible residues from Asp-111 to Ser-162. The critical residues were Asp-111, Gln-134, Phe-135, Arg-158, and Ser-161 (Table 1).

### 3.6. Potential coordinated interactions between SARS-CoV-2 and the plasma membrane of a host cell: key role of gangliosides in lipid rafts

Taken together, these data strongly supported the concept of a dual receptor/attachment model for SARS-CoV-2, the RBD domain being involved I ACE-2 receptor recognition, and the NTD interface responsible for finding a ganglioside-rich landing area (lipid raft) at the cell surface.

Such a dual receptor model, consistent with the topology of the SARS-CoV-2 spike, is proposed in Figure 8. With this model in mind, we will know study the potential effect of

CLQ and CLQ-OH, which, according to our molecular modeling data, have both a high affinity for sialic acids and gangliosides.

### 3.7. Molecular mechanism of CLQ and CLQ-OH antiviral effect: preventing SARS-CoV-2 spike access to cell surface gangliosides

With the aim to establish whether CLQ and CLQ-OH could prevent the attachment of SARS-CoV-2 to plasma membrane gangliosides, we superposed the initial NTD-GM1 complex with a drug-ganglioside complex (Figure 9). To improve clarity, the ganglioside is not presented in Figure 9. What we can see in this superposition is that the NTD and the drugs (CLQ-OH in this case) share the same spatial position when bound to GM1, so that GM1 cannot bind at the same time the viral protein and the drug. This is due to the fact that the NTD and the drugs (CLQ and CLQ-OH) bind to GM1 with a similar mechanism controlled by a dyad of functional interactions: a hydrogen bond and a geometrically perfect CH-π stacking interaction. In the case of the NTD, the hydrogen bond involves Asn-167, whereas the CH- π stacking is mediated by aromatic ring of Phe-135 (Figure 6b). On one hand, Asn-167 establishes a network of hydrogen bonds with the GalNAc residue of GM1. On the other hand, the flat aromatic ring of Phe-135 stacks onto the cycle of the Glc residue of GM1. In the case of CLQ and CLQ-OH, it is the nitrogen-containing ring of the drug that stacks onto the Glc ring (Figure 4c). Note that both the Phe-135 (in red) and the CLQ-OH (in green) rings are located at the same position (Figure 9). The other CLQ-OH molecule, which covers the tip of the sugar part of the ganglioside interacts with the GalNAc ganglioside (Figure 4b). When the NTD is bound to the ganglioside, we find the side chain of Asn-137 at this exact position (Figure 9). Thus, once two CLQ-OH (or two CLQ) molecules are bound to a ganglioside (Figure 4e and 4f), any binding of a SARS-Cov-2 spike to the same ganglioside is totally

prevented. The energy required to overcome this steric incompatibility could be estimated to 1000 $kJ.mol^{-1}$, which is far too high to occur.

### 3.8. Sequence alignment analysis of SARS-CoV-2 and related coronavirus: evolution of the ganglioside binding domain at critical amino acid residues

Since CLQ and CLQ-OH are potential therapies for SARS-CoV-2 infection, it is important to check whether the amino acid residues identified as critical for ganglioside binding are conserved among clinical isolates. The alignment of the 111-162 domain of 11 clinical isolates of SARS-CoV-2 from various origins (including Asia and USA) is shown in Figure 10). In this region, which contains the ganglioside binding domain identified in the present report, all amino acids are fully conserved. Interestingly, the motif is built like a giant consensus ganglioside-binding domain: a central region displaying the critical aromatic residue (Phe-135) and a basic residue at each ending (Lys-113 and Arg-158). In the middle of each stretch separating this typical triad, there is a N-glycosylation site (Asn-122 and Asn-149). These regions are not directly involved in ganglioside binding, so that the oligosaccharide linked to these asparagine residues could be perfectly intercalated between the sugar headgroup of gangliosides.

We also noted that the ganglioside binding domain of the NTD is fully conserved in the Bat RaTG13, which indicates a close relationship between the bat coronavirus and the human isolates that are currently circulating over the world. However, the motif is slightly different in other bat and human related coronaviruses (Figure 10), suggesting a recent evolution which could explain, at least in part, why SARS-CoV-2 is more contagious than previously characterized human coronaviruses.

## 4. Discussion

Sialic acids linked to glycoproteins and gangliosides are used by a broad range of viruses as receptors and/or attachment factors for cell entry [10]. These viruses include major human pathogens affecting the respiratory tract such as influenza [21] and corona viruses [22,23]. The attachment to sialic acid-containing cell surface structures is mediated by receptor binding proteins that belong to the viral spike. In the case of coronaviruses, this function is fulfilled by the spike (S) glycoprotein [9, 24]. SARS-CoV and SARS-CoV-2 interact with the ACE-2 protein, which has been identified as a key determinant of virus contagiousness [8]. However, considering the increased transmissibility of SARS-CoV-2 relative to SARS-CoV, binding to ACE-2 alone might not be enough to ensure a robust infection of the upper respiratory tract. Thus, it is likely that the new virus might also bind to other cell surface attachment factors, such as sialic acid-containing glycoproteins and gangliosides. Consistent with this notion, it has been shown that depletion of cell surface sialic acids by neuraminidase treatment inhibited MERS-CoV entry of human airway cells [25]. These data, which provided direct evidence that sialic acids play a critical role in human coronavirus attachment, broaden the therapeutic options to block the replication of the new virus SARS-CoV-2 that is responsible for the COVID-19 pandemic.

There are not many drugs that showed consistent antiviral efficiency in vitro together with reported efficiency in SARS-CoV-2 infected patients [3, 12]. One of them, CLQ, has retained our attention because its chemical structure is based on a combination of cationic nitrogen atoms and aromatic rings. Both features have been previously demonstrated as key determinants of sialic acid and ganglioside recognition by proteins [20, 26]. Our modeling approaches have been successfully used to decipher various molecular mechanisms of protein-sugar interactions accounting for the interaction of virus [27], bacterial [28], membrane [13] and amyloid proteins [20] with cell surface glycolipids. We applied this in

silico strategy to unravel the molecular mechanisms underlying the antiviral mechanisms of CLQ against SARS-CoV-2 infections. First, we showed that CLQ and CLQ-OH readily bind to isolated sialic acids with high affinity, including the typical 9-O-SIA subtype recognized by coronavirus [23]. Then, we showed that CLQ and CLQ-OH also bind to sialic acid-containing gangliosides. Based on these data, one can anticipate that the drugs might also recognize the sialic acid residues of glycoproteins. Further studies will help clarify this point.

Our molecular modeling studies led us to identify of a new type of ganglioside binding domain in the NTD of the SARS-CoV-2 S protein. This ganglioside binding domain consists of a large flat interface enriched in aromatic and basic amino acid residues. It covers 52-amino acid residues stretch (aa 111-162), which is definitely longer than all linear ganglioside binding domains characterized so far [29]. However, the new SARS-CoV-2 motif is organized in three distinct regions including a central aromatic domain and two terminal basic domains (Figure 10). Thus, this motif displays the typical features that determine an optimal binding to gangliosides, i.e. CH-π stacking and electrostatic interactions.

A major outcome of our study is the demonstration that CLQ and CLQ-OH display molecular groups that fully mimic the way the S viral protein binds to gangliosides. Two CLQ (or two CLQ-OH) molecules can simultaneously bind to the polar head group of ganglioside GM1. Interestingly, our simulations indicated that CLQ-OH is clearly more potent than CLQ, in line with the reported increased antiviral activity of CLQ-OH against SARS-CoV-2 [30]. Once bound to GM1, the drugs prevent any access to the Glc and GalNAc units the ganglioside, which are the critical binding residues for Phe-135 and Asn-137, respectively. This amino acid dyad, as well as all the other residues that mediate ganglioside binding by the SARS-CoV-2 spike, is fully conserved among clinical isolates worldwide. It is also conserved in the bat RaTG13isolate, which reinforces the hypothesis of a bat-to-human transmission. From the epidemiology point of view, it can be hypothesized that the evolution of this motif has

conferred an enhanced attachment capacity of human coronavirus to the respiratory tract, through improved spike-ganglioside interactions.

## 5. Conclusion

In face of the worldwide health emergency, drug repurposing is obviously the option of choice [2,3]. However, we could save a lot of time by testing in silico the capability of any potential anti-SARS-CoV-2 to block the very first step of the viral cycle. Applied to both RBD-ACE-2 and NTD-ganglioside interactions, our molecular modeling method will help selecting those drugs that are likely to interfere with the initial attachment of virus particles to the respiratory tract surface epithelium. In any case, our data do support the use of CLQ and preferentially CLQ-OH as a first intention therapy for patients infected with SARS-CoV-2.

## 6. References

[1] Zhou P, Yang XL, Wang XG, Hu B, Zhang L, Zhang W, et al. A pneumonia out- break associated with a new coronavirus of probable bat origin. Nature 2020; 579:270–273. doi: 10.1038/s41586-020-2012-7

[2] Mullard A. Drug repurposing programmes get lift off. Nat Rev Drug Discov 2012;11:505–6. doi: 10.1038/nrd3776

[3] Colson P, Rolain JM, Raoult D. Chloroquine for the 2019 novel coronavirus SARS-CoV-2. Int J Antimicrob Agents. 2020; 55:105923. doi:10.1016/j.ijantimicag.2020.105923

[4] Gao J, Tian Z, Yang X. Breakthrough: Chloroquine phosphate has shown apparent efficacy in treatment of COVID-19 associated pneumonia in clinical studies. Biosci Trends. 2020 Feb 19. doi:10.5582/bst.2020.01047 [Epub ahead of print]

[5] Savarino A, Di Trani L, Donatelli I, Cauda R, Cassone A. New insights into the antiviral effects of chloroquine. Lancet Infect Dis 2006; 6:67-69.

doi:10.1016/S1473-3099(06)70361-9

[6] Mauthe M, Orhon I, Rocchi C, Zhou X, Luhr M, Hijlkema KJ, Coppes RP, Engedal N, Mari M, Reggiori F. Chloroquine inhibits autophagic flux by decreasing autophagosome-lysosome fusion. Autophagy. 2018;14:1435-1455. doi:10.1080/15548627.2018.1474314

[7] Vincent MJ, Bergeron E, Benjannet S, Erickson BR, Rollin PE, Ksiazek TG, et al. Chloroquine is a potent inhibitor of SARS coronavirus infection and spread. Virol J 2005;2:69. doi:10.1186/1743-422X-2-69

[8] Li W, Moore MJ, Vasilieva N, Sui J, Wong SK, Berne MA, Somasundaran M, Sullivan JL, Luzuriaga K, Greenough TC, Choe H, Farzan M. Angiotensin-converting enzyme 2 is a functional receptor for the SARS coronavirus. Nature. 2003; 426: 450-454. doi: 10.1038/nature02145

[9] Yan R, Zhang Y, Li Y, Xia L, Guo Y, Zhou Q. Structural basis for the recognition of the SARS-CoV-2 by full-length human ACE2. Science. 2020 Mar 4. pii: eabb2762. doi:10.1126/science.abb2762 [Epub ahead of print]

[10] Matrosovich M, Herrler G, Klenk HD. Sialic Acid Receptors of Viruses. Top Curr Chem. 2015;367:1-28. doi:10.1007/128_2013_466

[11] Di Scala C, Fantini J. Hybrid In Silico/In Vitro Approaches for the Identification of Functional Cholesterol-Binding Domains in Membrane Proteins. Methods Mol Biol. 2017;1583:7-19. doi: 10.1007/978-1-4939-6875-6_2.

[12] Colson P, Rolain JM, Lagier JC, Brouqui P, Raoult D. Chloroquine and hydroxychloroquine as available weapons to fight COVID-19. Int J Antimicrob Agents. 2020 Mar 4:105932. doi: 10.1016/j.ijantimicag.2020.105932. [Epub ahead of print]

[13] Flores A, Ramirez-Franco J, Desplantes R, Debreux K, Ferracci G, Wernert F, Blanchard MP, Maulet Y, Youssouf F, Sangiardi M, Iborra C, Popoff MR, Seagar M, Fantini J, Lévêque C, El Far O. Gangliosides interact with synaptotagmin to form the high-affinity receptor complex for botulinum neurotoxin B. Proc Natl Acad Sci U S A. 2019;116(36):18098-18108. doi: 10.1073/pnas.1908051116.

[14] Huang Y, Huang S, Di Scala C, Wang Q, Wandall HH, Fantini J, Zhang YQ. The glycosphingolipid MacCer promotes synaptic bouton formation in Drosophila by interacting with Wnt. Elife. 2018;7. pii: e38183. doi: 10.7554/eLife.38183.

[15] Lee J, Patel DS, Ståhle J, Park SJ, Kern NR, Kim S, Lee J, Cheng X, Valvano MA, Holst O, Knirel YA, Qi Y, Jo S, Klauda JB, Widmalm G, Im W. CHARMM-GUI Membrane Builder for Complex Biological Membrane Simulations with Glycolipids and Lipoglycans. J Chem Theory Comput. 2019;15:775-786. doi: 10.1021/acs.jctc.8b01066.

[16] Wrapp D, Wang N, Corbett KS, Goldsmith JA, Hsieh CL, Abiona O, Graham BS, McLellan JS. Cryo-EM structure of the 2019-nCoV spike in the prefusion conformation. Science. 2020;367:1260-1263. doi: 10.1126/science.abb2507.

[17] Guvench O, Greene SN, Kamath G, Brady JW, Venable RM, Pastor RW, Mackerell AD Jr. Additive empirical force field for hexopyranose monosaccharides. J Comput Chem. 2008; 29:2543-2564. doi: 10.1002/jcc.21004.

[18] Park YJ, Walls AC, Wang Z, Sauer MM, Li W, Tortorici MA, Bosch BJ, DiMaio F, Veesler D. Structures of MERS-CoV spike glycoprotein in complex with sialoside attachment receptors. Nat Struct Mol Biol. 2019;26:1151-1157. doi: 10.1038/s41594-019-0334-7.

[19] The Lysosomal Protein Saposin B Binds Chloroquine. Huta BP, Mehlenbacher MR, Nie Y, Lai X, Zubieta C, Bou-Abdallah F, Doyle RP. ChemMedChem. 2016;11:277-382. doi: 10.1002/cmdc.201500494.

[20] Yahi N, Fantini J. Deciphering the glycolipid code of Alzheimer's and Parkinson's amyloid proteins allowed the creation of a universal ganglioside-binding peptide. PLoS One. 2014;9:e104751. doi: 10.1371/journal.pone.0104751.

[21] Verma DK, Gupta D, Lal SK. Host Lipid Rafts Play a Major Role in Binding and Endocytosis of Influenza A Virus. Viruses. 2018;10. pii: E650. doi: 10.3390/v10110650.

[22] Lu Y, Liu DX, Tam JP. Lipid rafts are involved in SARS-CoV entry into Vero E6 cells. Biochem Biophys Res Commun. 2008;369:344-349. doi: 10.1016/j.bbrc.2008.02.023.

[23] Tortorici MA, Walls AC, Lang Y, Wang C, Li Z, Koerhuis D, Boons GJ, Bosch BJ, Rey FA, de Groot RJ, Veesler D. Structural basis for human coronavirus attachment to sialic acid receptors. Nat Struct Mol Biol. 2019; 26: 481-489. doi: 10.1038/s41594-019-0233-y.

[24] Hoffmann M, Kleine-Weber H, Schroeder S, Krüger N, Herrler T, Erichsen S, Schiergens TS, Herrler G, Wu NH, Nitsche A, Müller MA, Drosten C, Pöhlmann S. SARS-CoV-2 Cell Entry Depends on ACE2 and TMPRSS2 and Is Blocked by a Clinically Proven Protease Inhibitor. Cell. 2020; pii: S0092-8674(20)30229-4. doi: 10.1016/j.cell.2020.02.052. [Epub ahead of print]

[25] Li W, Hulswit RJG, Widjaja I, Raj VS, McBride R, Peng W, Widagdo W, Tortorici MA, van Dieren B, Lang Y, van Lent JWM, Paulson JC, de Haan CAM, de Groot RJ, van Kuppeveld FJM, Haagmans BL, Bosch BJ. Identification of sialic acid-binding function for the Middle East respiratory syndrome coronavirus spike glycoprotein. Proc Natl Acad Sci U S A. 2017;114: E8508-E8517. doi: 10.1073/pnas.1712592114.

[26] Fantini J, Yahi N. Molecular insights into amyloid regulation by membrane cholesterol and sphingolipids: common mechanisms in neurodegenerative diseases. Expert Rev Mol Med. 2010;12:e27. doi: 10.1017/S1462399410001602.

[27] Mahfoud R, Garmy N, Maresca M, Yahi N, Puigserver A, Fantini J. Identification of a common sphingolipid-binding domain in Alzheimer, prion, and HIV-1 proteins. J Biol Chem. 2002; 277: 11292-11296. doi: 10.1074/jbc.M111679200.

[28] Fantini J, Garmy N, Yahi N. Prediction of glycolipid-binding domains from the amino acid sequence of lipid raft-associated proteins: application to HpaA, a protein involved in the adhesion of Helicobacter pylori to gastrointestinal cells. Biochemistry. 2006;45:10957-10962. doi: 10.1021/bi060762s

[29] Fantini J, Yahi N. Brain Lipids in Synaptic Function and Neurological Disease. Clues to Innovative Therapeutic Strategies for Brain Disorders. Elsevier Academic Press; San Francisco: 2015. ISBN: 9780128001110.

[30] Yao X, Ye F, Zhang M, Cui C, Huang B, Niu P, Liu X, Zhao L, Dong E, Song C, Zhan S, Lu R, Li H, Tan W, Liu D. In Vitro Antiviral Activity and Projection of Optimized Dosing Design of Hydroxychloroquine for the Treatment of Severe Acute Respiratory Syndrome Coronavirus 2 (SARS-CoV-2). Clin Infect Dis. 2020 Mar 9. pii: ciaa237. doi: 10.1093/cid/ciaa237.

**Figure legends**

**Figure 1. Chemical structure of chloroquine (CLQ) and hydroxychloroquine (CLQ-OH):**

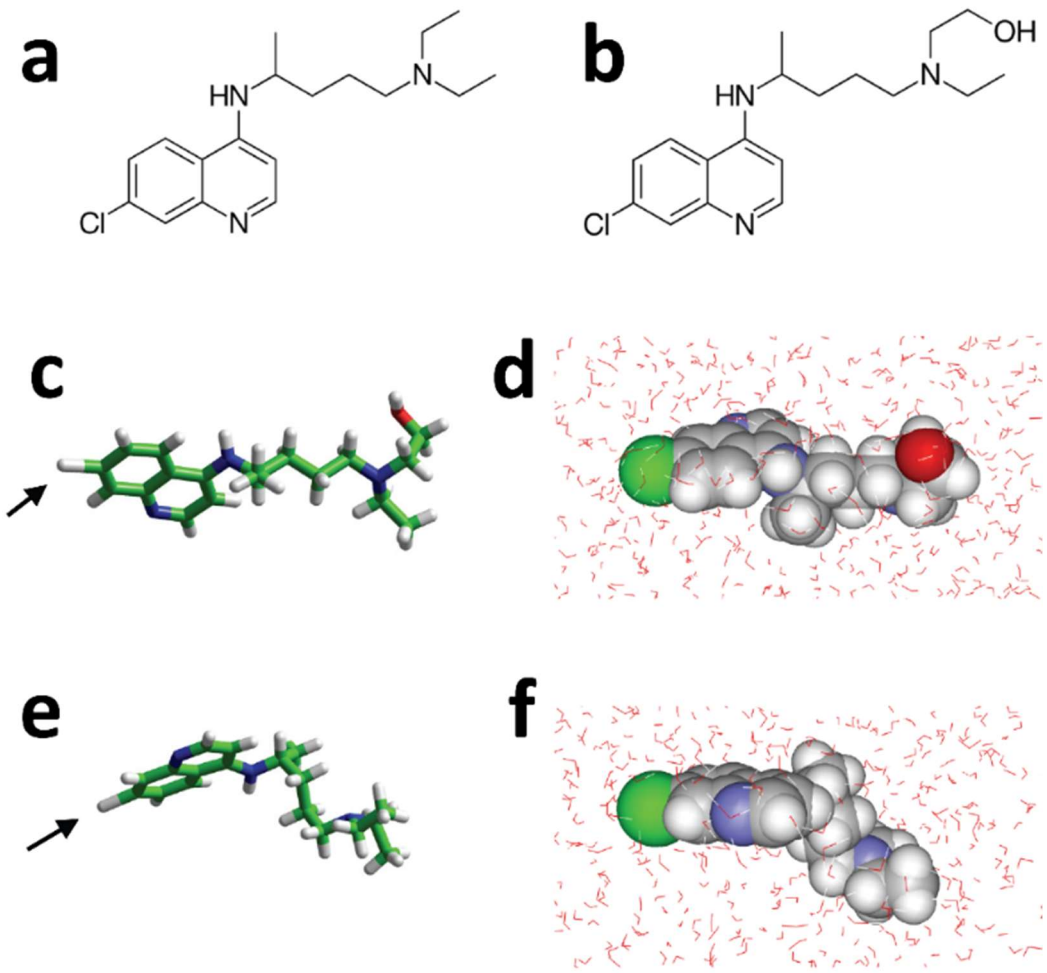


**a-** CLQ; **b-** CLQ-OH; **c-** CLQ-OH extended conformer; **d-** CLQ-OH in water; **e-** typical condensed conformer of CLQ; **f-** CLQ in water. The molecules in **c-f** panels are shown in either tube or sphere rendering (carbon green, nitrogen blue, oxygen red, hydrogen white). In panels **c** and **e**, the chlorine atom of CLQ and CLQ-OH is indicated by an arrow.

**Figure 2. Molecular modeling of CLQ interaction with sialic acids:**

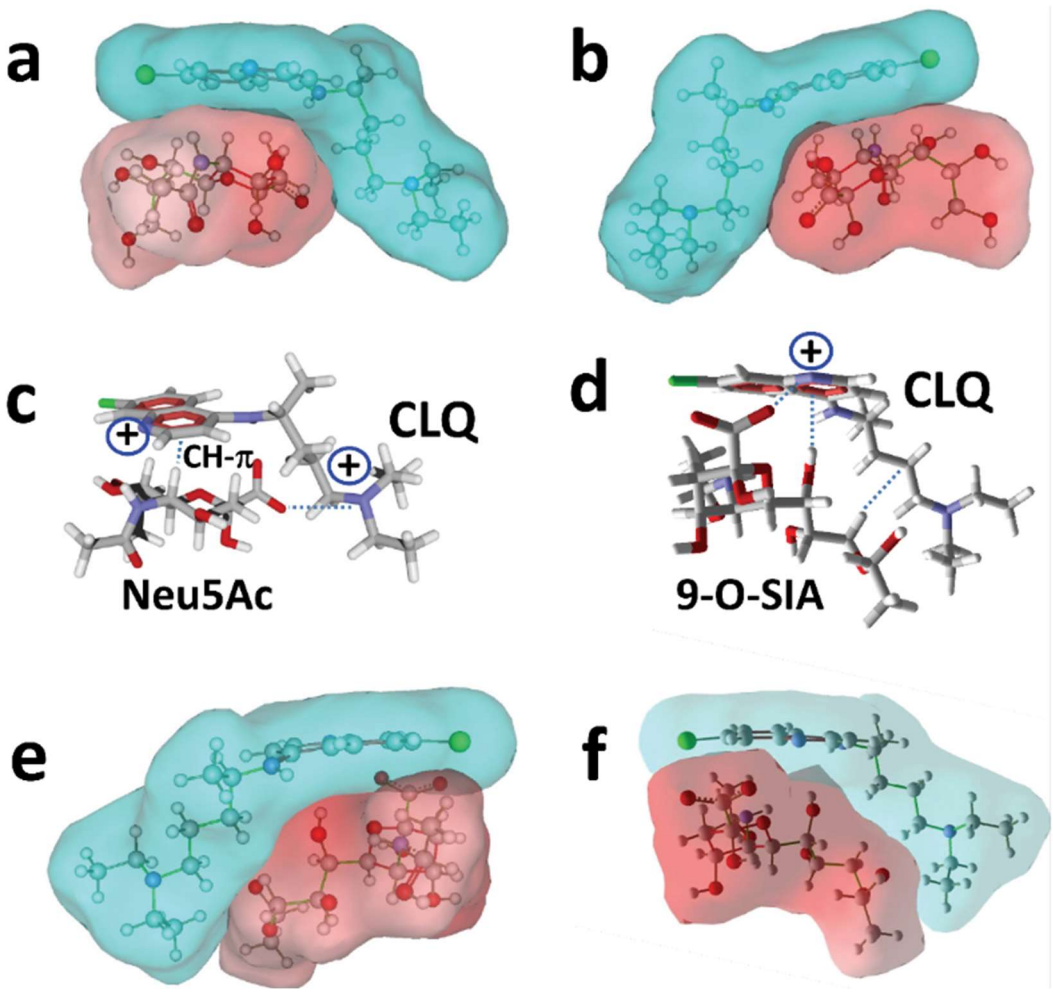


**a,b-** surface representation of the CLQ-sialic acid (Neu5Ac) complex. Two opposite views of the complex are shown. Note the geometric complementarity between the L-shape conformer of chloroquine dissolved in water (in blue) and Neu5Ac (in red);**c-** sialic acid (Neu5Ac) bound to CLQ via a combination of CH-π and electrostatic interactions with one of the cationic group of CLQ (+); **d-** molecular modeling of CLQ bound to N-Acetyl-9-O-acetylneuraminic acid (9-O-SIA). From the right to the left, the dashed lines indicate a series of van der Waals, OH-π and electrostatic contacts with both cationic groups of CLQ (+); **e,f-** surface representations of the CLQ-9-O-SIA complex.

**Figure 3. Molecular modeling of CLQ-OH interaction with sialic acids:**

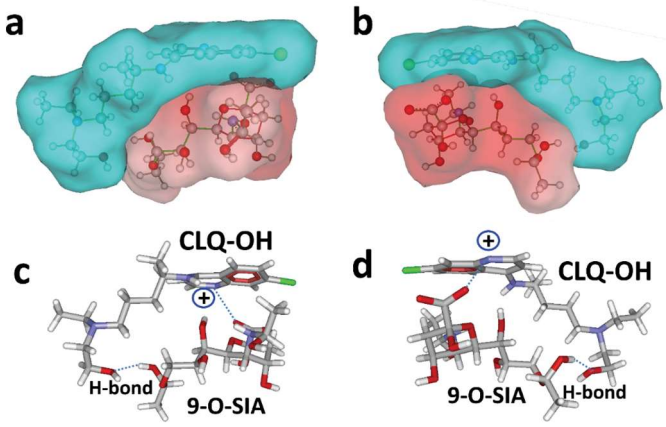


**a,b-** surface representation of the CLQ-OH bound to 9-O-SIA. Two opposite views of the complex are shown. Note the geometric complementarity between CLQ-OH (in blue) and (9-O-SIA) (in red); **c,d-** molecular mechanism of CLQ-OH binding to 9-O-SIA: combination of electrostatic interactions and hydrogen bonding.

**Figure 4. Molecular modeling simulations of CLQ and CLQ-OH binding to ganglioside GM1:**

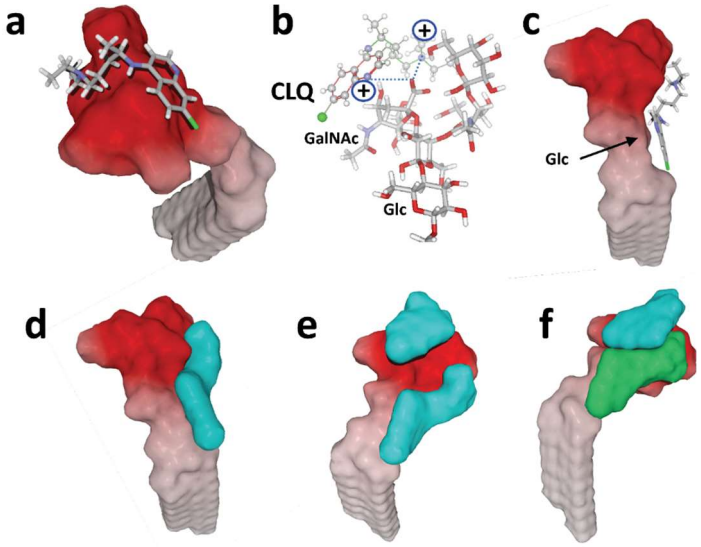


the surface electrostatic potential of GM1 indicates a nonpolar, membrane embedded part corresponding to ceramide (white areas), and an acidic part protruding in the extracellular space corresponding to the sialic acid containing saccharide part (red areas). **a-** CLQ bound to the tip of the carbohydrate moiety of GM1; **b-** molecular mechanism of CLQ-ganglioside interactions; **c-** molecular dynamics simulations revealed a second site of interaction. In this case, the aromatic cycles of CLQ are positioned at the ceramide-sugar junction whereas the nitrogen atoms interact with the acidic part of the ganglioside (not illustrated here for clarity purpose); **d-e** surface views of GM1 complexed with one (**d**) or two (**e**) CLQ molecules (both in blue), illustrating the geometric complementarity of GM1 and CLQ molecules; **f-** one GM1 molecule can also accommodate simultaneously two distinct CLQ-OH molecules, after a slight rearrangement allowing an increased fit due CLQ-OH /CLQ-OH interactions. To improve clarity, the CLQ-OH bound to GM1 are represented in two distinct colors (blue and green).

**Figure 5. Structural features of the SARS-CoV-2 spike protein:**

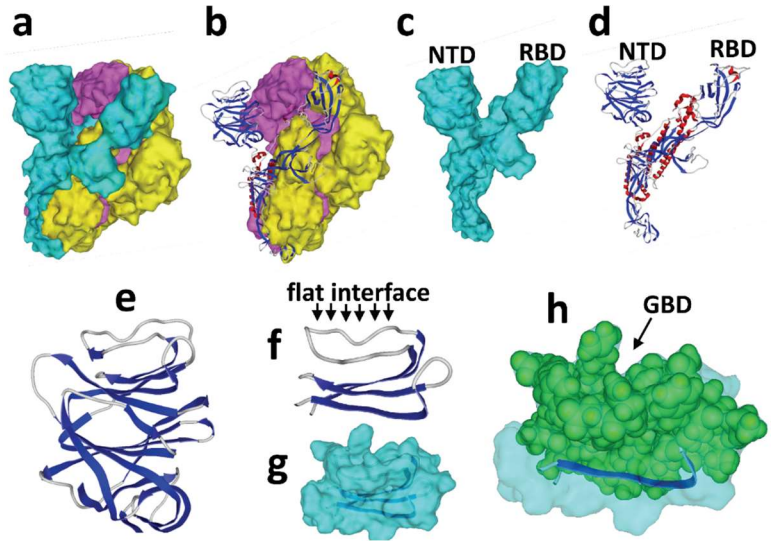


**a-**trimeric structure (each S protein has a distinct surface color, "blue", "yellow" and "purple"); **b-** ribbon representation of "blue" S protein in the trimer (α-helix in red, β-strand in blue, coil in grey); **c-** surface structure of the "blue" S protein isolated from the trimer; **d-** ribbon structure of the "blue" S protein; **e-** zoom on the NTD domain of the "blue" S protein; **f,g-** molecular model of a minimal NTD obtained with Hyperchem (ribbon in representation in **f**, surface rendering in **g**); **h-** highlighting of the amino acid residues of the NTD that could be belong to a potential ganglioside binding domain (GBD).

**Figure 6. Molecular complex between the NTD of SARS-CoV-2 S protein and a single GM1 ganglioside:**

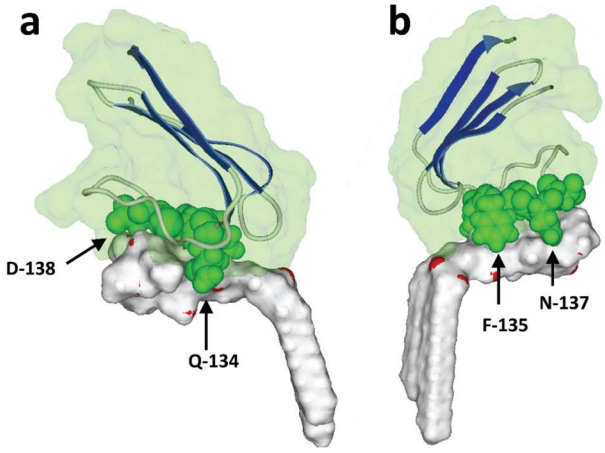


the NTD is represented in ribbons superposed with a transparent surface rendering (light green). Two symmetric views of the complex are shown (panels **a** and **b**). The amino acid residues Q-134 to D-138 located in the center of the ganglioside binding domain (GBD) are represented in green spheres. The saccharide part of the ganglioside forms a landing surface for the tip of the NTD.

**Figure 7. Molecular complex between the NTD of SARS-CoV-2 S protein and a dimer of GM1:**

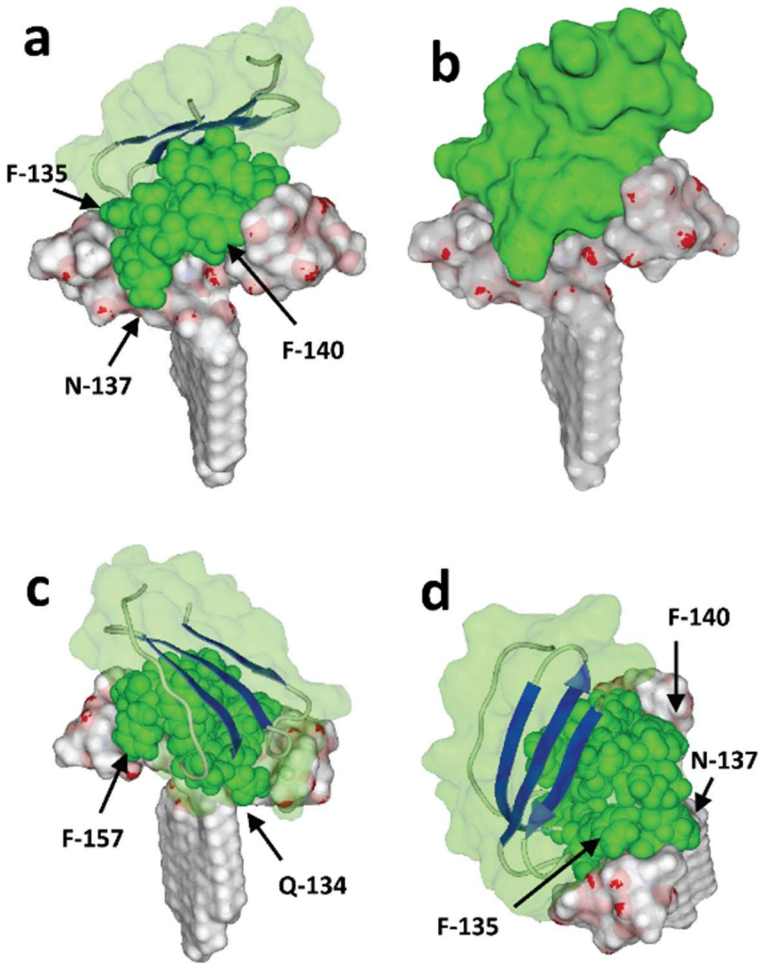


in panels **a**, **c** and **d**, **the** NTD is represented as in Figure 4. In panel **b**, the surface of the NTD is shown without any transparency. The amino acid residues Q-134 to S-162 belonging to the GBD are represented in green spheres. Compared with a single GM1 molecule, the dimer of gangliosides forms a larger attractive surface for the NTD. In the above view of panel **d**, the anchorage of the NTD to the gangliosides is particularly obvious. Since CLQ also interacts with the saccharide part of GM1, its presence would clearly mask most of the landing surface available for the NTD, preventing the primary attachment of the virus to the plasma membrane of host cells.

**Figure 8. Dual recognition of gangliosides and ACE-2 by SARS-CoV-2 S protein:**

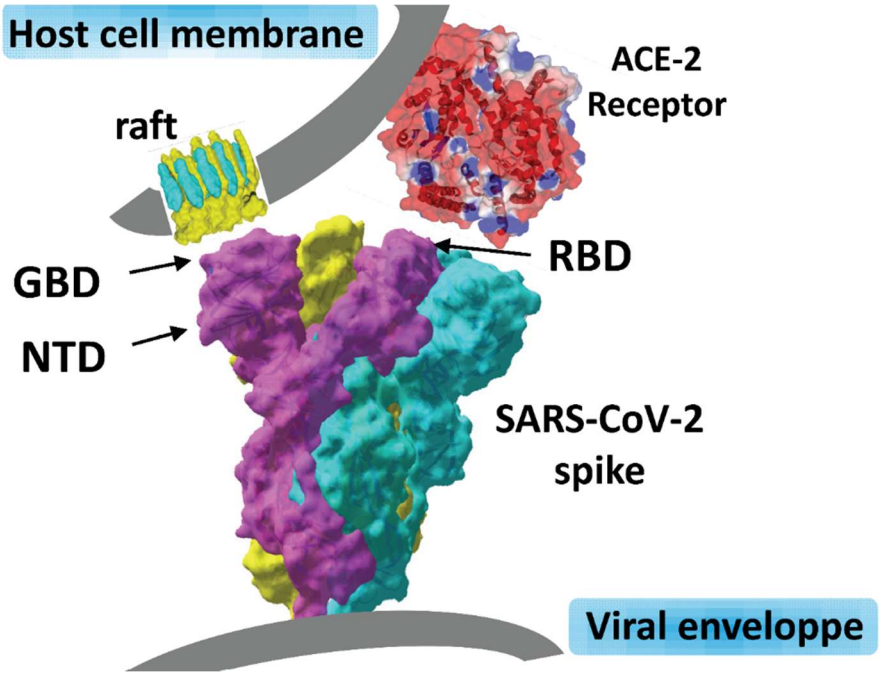


the viral protein displays two distinct domains whose tips are available for distinct types of interactions. The RBD binds to the ACE-2 receptor, and the NTD with ganglioside-rich domain of the plasma membrane. Lipid rafts, which are membrane domains enriched in gangliosides (in yellow) and cholesterol (in blue), provide a perfect attractive interface for adequately positioning the viral spike at the earliest step of the infection process. Our structural and molecular modeling studies suggest that the amino acid residues 111-162 of the NTD form a functional ganglioside binding domain (GBD) whose interaction with lipid rafts can be efficiently prevented by CLQ and CLQ-OH.

**Figure 9. Mechanism of action of CLQ and CLQ-OH:**

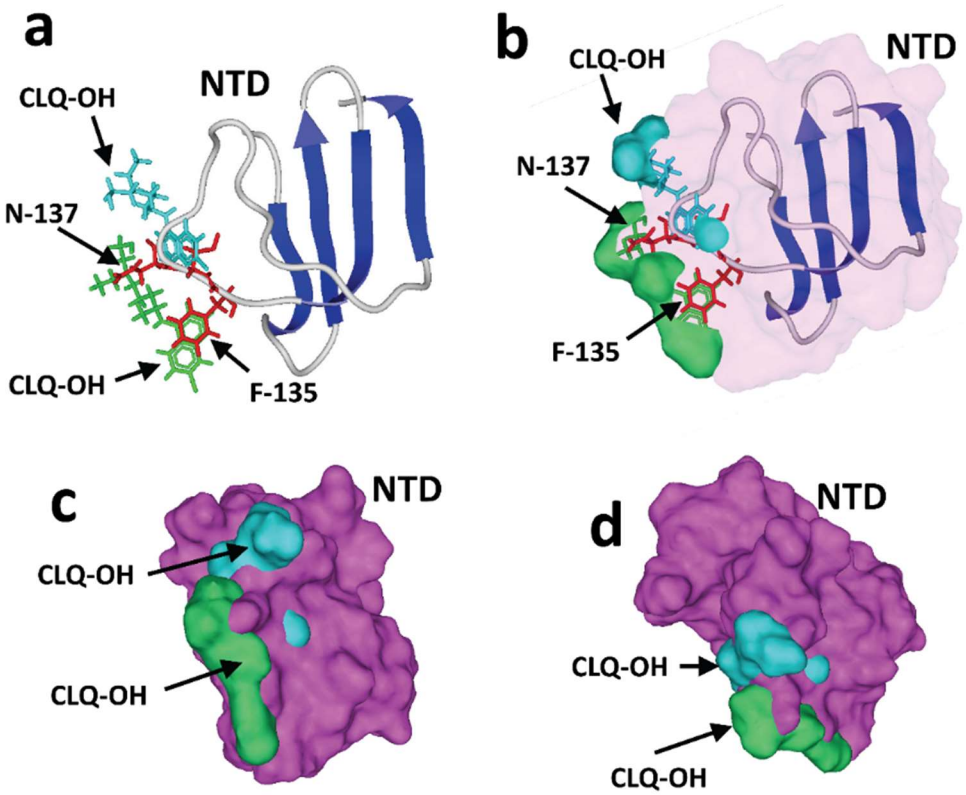


the NTD bound to GM1 was superposed onto GM1 in interaction with two CLQ-OH molecules. The models show only the NTD and both CLQ-OH molecules (and not GM1 to improve clarity). **a,b-** the aromatic ring of F-135 (in red) , which stacks onto the Glc cycle of GM1 overlaps the aromatic CLQ-OH rings (in green) which also binds to GM1 via a CH-π stacking mechanism. The N-137 residue of the NTD interacts with the GalNAc residue of GM1 but in presence of CLQ-OH this interaction cannot occur as this part of GM1 is totally masked by the drug; **c,d-** superposition of the NTD surface (in purple) with the two CLQ-OH molecules bound to GM1, illustrating the steric impossibility that totally prevents NTD binding to GM1 when both CLQ-OH molecules are already interacting with the ganglioside.

**Figure 10. Amino acid sequence alignments of the ganglioside binding domain of the SARS-CoV-2 S protein:**

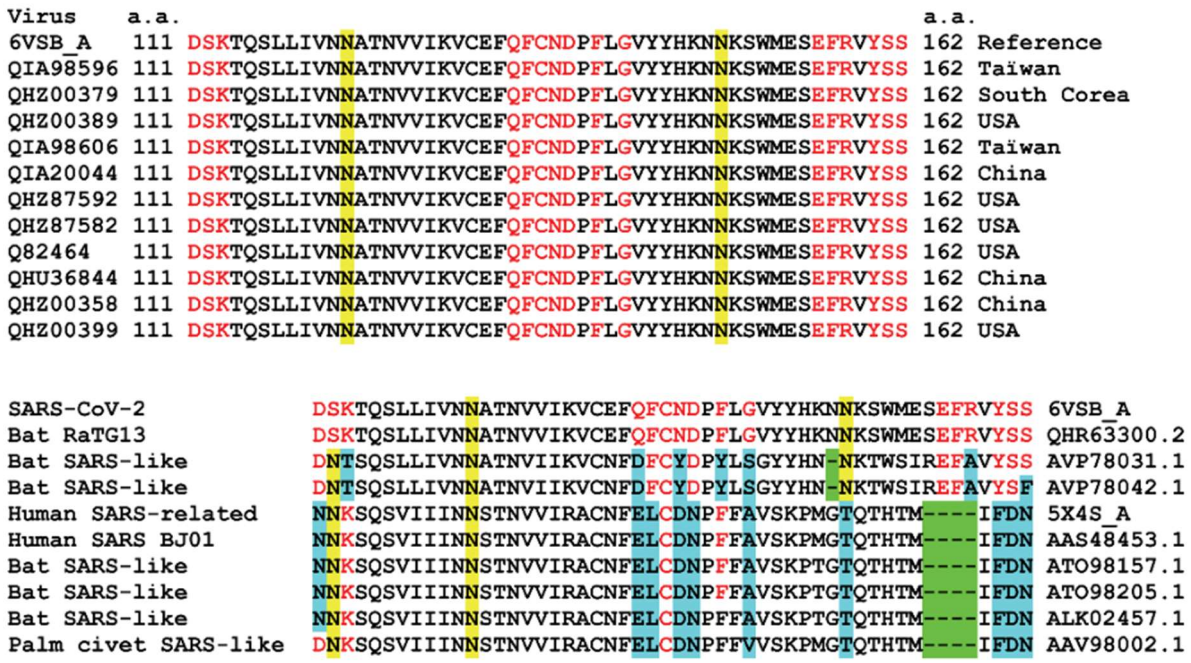


**a-** clinical SARS-CoV-2 isolates aligned with the reference sequence (6VSB_A, fragment 111-162). The amino acid residues involved in GM1 binding are indicated in red. Two asparagine residues acting as glycosylation sites are highlighted in yellow; **b-** alignments of human and animal viruses compared with SARS-CoV-2 (6VSB_A, fragment 111-162). Deletions are highlighted in green, amino acid changes in residues involved in ganglioside binding are highlighted in blue. Conserved residues are in red. Asparagine residues acting as glycosylation sites are highlighted in yellow.

**Table 1. Energy of interaction of each amino acid residue of SARS-CoV-2 spike protein in contact with GM1 molecules.**

| *Amino acid residues* | *Energy of interaction (in kJ.mol$^{-1}$)* |
|---|---|
| **Initial step: 1 GM1 molecule** | |
| Asp-111 | - 5.6 |
| Lys-113 | - 8.2 |
| Gln-134 | - 8.6 |
| Phe-135 | - 20.1 |
| Cys-136 | - 7.0 |
| Asn-137 | - 15.2 |
| Asp-138 | - 6.4 |
| Arg-158 | - 17.4 |
| Ser-161 | - 9.7 |
| Ser-162 | - 2.0 |
| **Total** | **-100.2** |
| **2$^{nd}$ step: 2 GM1 molecules** | |
| Asp-111 | - 15.8 |
| Ser-112 | - 10.7 |
| Lys-113 | - 9.2 |
| Gln-134 | - 11.2 |
| Phe-135 | - 10.5 |
| Cys-136 | - 6.2 |
| Asn-137 | - 4.7 |
| Phe-140 | - 5.2 |
| Gly-142 | - 5.6 |
| Glu-156 | - 9.0 |
| Phe-157 | - 13.8 |
| Arg-158 | - 19.8 |
| Tyr-160 | - 3.2 |
| Ser-161 | - 9.7 |
| Ser-162 | - 2.0 |
| **Total** | **-137.6** |